

Investigation of the Microstructure and Chemical Composition of $\text{CaCu}_3\text{Ti}_4\text{O}_{12}$ Multilayer Elements using SEM, EDS, and XPS

A. SKWAREK^{a,*}, R.P. SOCHA^b, D. SZWAGIERCZAK^a AND P. ZACHARIASZ^a

^aInstitute of Electron Technology, Kraków Division, Zabłocie 39, 30-701 Kraków, Poland

^bInstitute of Catalysis and Surface Chemistry, Polish Academy of Sciences, Niezapominajek 8, 30-239 Krakow, Poland

In this paper the microstructure and chemical composition of $\text{CaCu}_3\text{Ti}_4\text{O}_{12}$ multilayer elements fabricated using low temperature cofired ceramics procedure were characterized by scanning electron microscope, energy dispersive spectroscopy and X-ray photoelectron spectroscopy. The multilayer elements were obtained in the process encompassing: tape casting, laser cutting, screen printing, isostatic lamination and cofiring of ceramic tapes with internal conductive films at 940 °C. The compatibility of $\text{CaCu}_3\text{Ti}_4\text{O}_{12}$ with three commercial Ag and Ag–Pd thick film pastes was confirmed. The results of scanning electron microscope and energy dispersive spectroscopy analysis revealed close to the stoichiometric composition of $\text{CaCu}_3\text{Ti}_4\text{O}_{12}$ grains and significant enrichment in oxygen of grain boundaries. X-ray photoelectron spectroscopy studies showed that main oxidation states of the component elements were Cu^{2+} , Ti^{4+} , and Ca^{2+} .

DOI: [10.12693/APhysPolA.134.318](https://doi.org/10.12693/APhysPolA.134.318)

PACS/topics: calcium copper titanate, low temperature cofired ceramics, SEM analysis, EDS analysis, XPS analysis

1. Introduction

$\text{CaCu}_3\text{Ti}_4\text{O}_{12}$ [1–3] and other compounds with the similar perovskite crystal structure, like $\text{Bi}_{2/3}\text{Cu}_3\text{Ti}_4\text{O}_{12}$, $\text{Cu}_2\text{Ta}_4\text{O}_{12}$, $\text{Dy}_{2/3}\text{CuTa}_4\text{O}_{12}$ [4–7] exhibit promising dielectric and electric behavior. High dielectric constant and nonlinear current–voltage characteristics exhibited by these materials originate from spontaneous formation of internal barrier layers, mainly at grain boundaries. Potential applications of $\text{CaCu}_3\text{Ti}_4\text{O}_{12}$ -type compounds in low temperature cofired ceramics (LTCC) multilayer electronic components, like capacitors and varistors, have not been so far intensively investigated [8–11].

In this work, applicability of LTCC technology for fabrication of $\text{CaCu}_3\text{Ti}_4\text{O}_{12}$ based multilayer structures was examined. Characterization of the microstructure and elemental composition of the prepared samples was performed using scanning electron microscopy (SEM), energy dispersive spectroscopy (EDS) and X-ray photoelectron spectroscopy (XPS).

2. Materials and equipments

The LTCC procedure used for fabrication of multilayer structures based on $\text{CaCu}_3\text{Ti}_4\text{O}_{12}$ consists of several steps: preparation of slurries, tape casting, laser

cutting of green tapes, screen printing of internal electrodes, stacking of green sheets, isostatic lamination, deposition of external contacts and cofiring of multilayer elements. Fine $\text{CaCu}_3\text{Ti}_4\text{O}_{12}$ powder was obtained as a result of the synthesis at 980 °C and subsequent grinding using a Fritsch ball mill. In order to prepare a slurry, the ceramic powder was mixed with organic additives: polyvinyl butyral as a binder, fish oil as a dispersant, polyethylene glycol and dibutyl phthalate as plasticizers, toluene and isopropyl alcohol as solvents. A Mistler tape caster was applied for obtainment of 80 μm thick green tapes. Three types of commercial thick film pastes, ESL Ag 9916, ESL AgPd 9638-HD-G and DuPont Ag 6142D, were utilized for deposition of internal electrodes onto the surface of green sheets using a Microtech screen printer. Several $\text{CaCu}_3\text{Ti}_4\text{O}_{12}$ based layers were stacked and pressed isostatically under a pressure of 40 MPa at 70 °C by means of a Pacific Trinetics Corporation laminator. The multilayer structures with internal electrodes connected in parallel were fired according to a profile which enabled slow burnout of organic components at about 300–450 °C and co-sintering of ceramic layers with metallic electrodes at 940 °C.

The grain size, compactness and cooperation of the ceramic layers with conductive thick films was studied by a scanning electron microscope (FEI, US). Elemental composition in the grain interiors, at the grain boundaries and at the ceramic layer–electrode interface was examined by energy dispersive spectroscopy.

Analysis of the elemental composition and electronic states of elements at the surface of the fractured sam-

*corresponding author; e-mail: askwarek@ite.waw.pl

ples was carried out by X-ray photoelectron spectroscopy (XPS). The electron binding energy (BE) of the core excitations generated by $\text{MgK}\alpha$ (1256.6 eV) or $\text{Al K}\alpha$ (1486.6 eV) radiation was examined by a hemispherical analyzer (SES R4000, Gammadata Scienta).

3. Results and discussion

Green tapes based on $\text{CaCu}_3\text{Ti}_4\text{O}_{12}$ after drying were smooth, defect-free, flexible, and demonstrate good mechanical strength. No delaminations or cracks were observed after isostatic pressing of the multilayer elements composed of 30 sheets with screen printed internal electrodes. As a result of cofiring, dense microstructure of $\text{CaCu}_3\text{Ti}_4\text{O}_{12}$ ceramic layers was attained. SEM images in Fig. 1a–c illustrate not uniform grain sizes in the range 0.5–7 μm , which give rise to the Maxwell–Wagner polarization, typical of this type of materials. The internal electrodes formed from all the applied commercial pastes cooperate well with the $\text{CaCu}_3\text{Ti}_4\text{O}_{12}$ ceramic layers. Cracks, bubbles, secondary phases were not found at

the phase boundary. Figure 1c presents the microstructure of the ceramic layer with the indicated points in which EDS analysis was carried out. The results of this analysis are shown in Table I.

The EDS analysis revealed that grains have composition close to the stoichiometric $\text{CaCu}_3\text{Ti}_4\text{O}_{12}$ with a slightly enhanced copper content related to Cu^+ ions. Relatively low sintering temperature of 940 $^\circ\text{C}$ is presumably the reason of low contribution of Cu^+ ions since intensive reduction of Cu^{2+} to Cu^+ is known to take place above 1030 $^\circ\text{C}$. The applied sintering temperature is also below the reported temperature of eutectic phase formation (about 1000 $^\circ\text{C}$) in the CuO – TiO_2 system [12]. A significant enrichment in oxygen was observed at grain boundaries. Higher Cu/O and Ti/O content ratios for $\text{CaCu}_3\text{Ti}_4\text{O}_{12}$ grains than for grain boundaries imply a higher concentration of Cu^+ and Ti^{3+} ions in grain interiors and a higher content of Cu^{2+} and Ti^{4+} ions at grain boundaries. This can lead to the formation of internal barrier layer effects in the material composed of semiconducting grains and insulating grain boundaries.

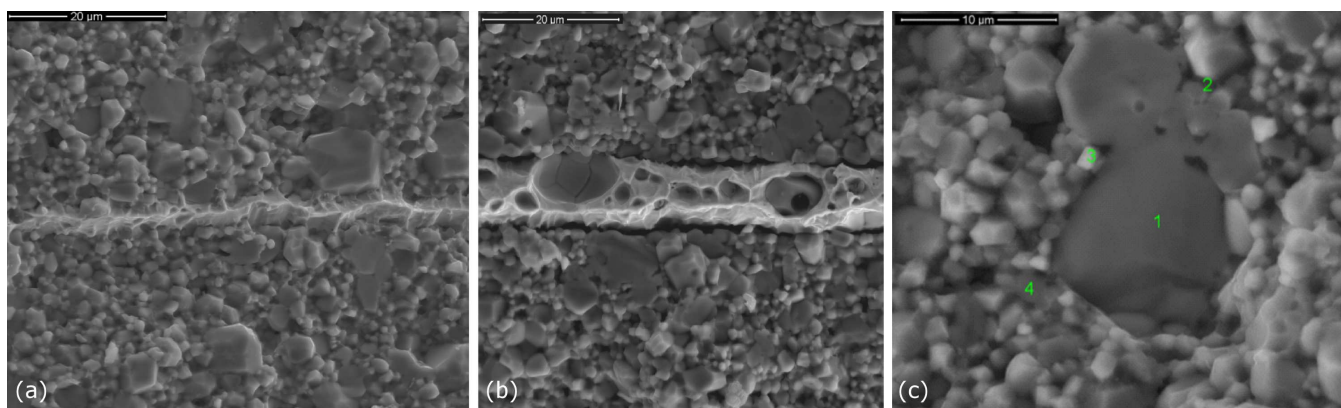


Fig. 1. SEM images of fractured cross-sections of $\text{CaCu}_3\text{Ti}_4\text{O}_{12}$ multilayer structures: (a) ceramic layer with ESL Ag electrode. Magnification 5000 \times , (b) ceramic layer with ESL AgPd electrode. Magnification 5000 \times , (c) ceramic layer with marked points of the EDS analysis (see Table I). Magnification 10000 \times .

XPS studies revealed that main oxidation states of the component elements are Ca^{2+} , Cu^{2+} , and Ti^{4+} . The sample surface was found to be enriched with copper and calcium as compared with the interior. Figure 2a–e illustrates the XPS spectra for the fractured $\text{CaCu}_3\text{Ti}_4\text{O}_{12}$ layers. The XPS spectrum for Ti 2p is illustrated in Fig. 2a. The component A of this spectrum with binding energy of 457.7 eV can be assigned to Ti^{4+} –O bond associated with Ti(IV) lattice species in Ti_4O_{12} anion. The component B is ascribed to Ti^{4+} –O bond related to Ti(IV) in mixed oxide anions. The binding energy corresponding to this component is 459.1 eV, this value being close to that reported for CaTiSiO_5 (459.6 eV) [13]. The surface and bulk content of titanium in the $\text{CaCu}_3\text{Ti}_4\text{O}_{12}$ sample was found to be similar.

Figure 2b presents O 1s spectrum. The component A with binding energy of 529.2 eV is attributed to O-metal bond, like for lattice oxygen in TiO_3^{2-} anion [14]

(similar to Ti_4O_{12} anion in $\text{CaCu}_3\text{Ti}_4\text{O}_{12}$). The component B (binding energy of 530.5 eV) is assigned to lattice oxygen for oxides+hydroxyl groups. The components C and D are related to organic compounds. The A component of the Ca 2p spectrum characterized by BE= 345.7 eV (Fig. 2c) can be assigned to Ca^{2+} –O bonded with Cu in a lattice of mixed oxides, e.g. like in $\text{Bi}_{1.6}\text{Pb}_{0.4}\text{Sr}_2\text{CaCu}_2\text{O}_{8+x}$ [15]. The component B (BE= 346.6 eV) corresponds to Ca^{2+} –O in CaO and/or $\text{Ca}(\text{OH})_2$. The sample surface was found to be enriched with Ca.

The component A of Cu 2p spectrum with binding energy of 933.4 eV (Fig. 2d) can be attributed to Cu^{2+} –O in CuO , while the component B with binding energy of 935.2 eV to Cu^{2+} –OH or Cu^{2+} –O in systems of CuAl_2O_4 , CuMoO_4 type (high electronegativity of environment). Use of the so-called modified Auger parameter ($\alpha' = \text{BE}(\text{Cu } 2p_{3/2}) + \text{KE}(\text{Cu } L_3M_{45}M_{45})$ Auger transition) en-

TABLE I

Results of the EDS analysis for $\text{CaCu}_3\text{Ti}_4\text{O}_{12}$ ceramic layers (in points 1–4 shown in Fig. 1c)

Element	Content [at.%]			
	1 - big dark grain	2 - grain boundary	3 - bright grain	4 - small dark grain
Ca	4.30	4.28	2.93	4.3
Cu	15.02	12.28	9.52	14.30
Ti	20.43	16.98	12.35	19.57
O	60.25	66.46	75.2	61.83
Cu/O	0.249	0.185	0.127	0.231
Ti/O	0.339	0.255	0.164	0.317
Cu/Ti	0.735	0.723	0.771	0.730
Cu/Ca	3.49	2.87	3.25	3.32

abled determination of oxidation state of the main component of copper spectrum. Binding energies (BE) and kinetic energies (KE) of Cu $L_3M_{45}M_{45}$ Auger peaks are obtained at the maxima of the excitations (Fig. 2e). The value of this parameter (1851.2 eV) indicates that the dominant oxidation state of copper in the investigated $\text{CaCu}_3\text{Ti}_4\text{O}_{12}$ samples is Cu^{2+} . The XPS studies did not prove directly the presence of Cu^+ ions. However, a distinct depletion in Cu (about 30%) of the surface in comparison with the sample bulk was observed which implies enhanced contribution of Cu^{2+} ions at the surface and possible presence of Cu^+ in the bulk.

4. Conclusion

Multilayer structures based on $\text{CaCu}_3\text{Ti}_4\text{O}_{12}$ ceramic, destined for multilayer capacitors or varistors, were prepared using LTCC technology. Basing on SEM observations, the microstructure of ceramic layers was found to be dense, with diverse grain sizes. Internal electrodes made of Ag and AgPd commercial pastes cooperated well with the $\text{CaCu}_3\text{Ti}_4\text{O}_{12}$ ceramic layers. As revealed by XPS studies, the main oxidation states of the component elements were Cu^{2+} , Ti^{4+} and Ca^{2+} . The EDS results well helpful in getting insight into the mechanism of creation of internal barrier layer effect, related to formation of semiconducting $\text{CaCu}_3\text{Ti}_4\text{O}_{12}$ grains enriched with Cu^+ and more resistive grain boundaries enriched in Cu^{2+} and oxygen.

Acknowledgments

The work has been financed by the National Science Centre, Poland, under the grant No. 2015/17/D/ST7/04141.

References

- [1] M.A. Subramanian, D. Li, N. Duan, B.A. Reisner, A.W. Sleight, *J. Solid State Chem.* **151**, 323 (2000).

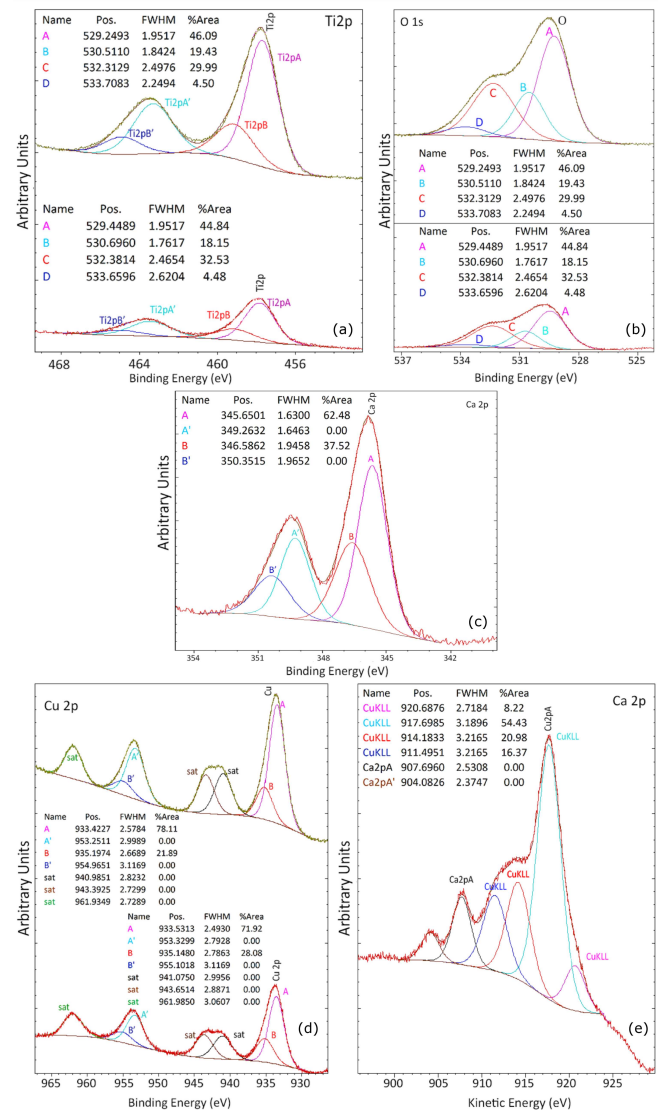


Fig. 2. The XPS spectra of a $\text{CaCu}_3\text{Ti}_4\text{O}_{12}$ fractured multilayer sample for Mg K_{α} (lower plots) and Al K_{α} (upper plots) radiation: (a) Ti 2p, (b) O 1s, (c) Ca 2p (Al K_{α} radiation), (d) Cu 2p, (e) Cu KLL (Auger spectrum) and Ca 2p (XPS spectrum — Mg K_{α} radiation).

- [2] D.C. Sinclair, T.B. Adams, F.D. Morrison, A.R. West, *Appl. Phys. Lett.* **80**, 2153 (2002).
- [3] X. Zhao, L. Ren, R. Liao, J. Li, L. Yang, *J. Electron. Mater.* **45**, 3079 (2016).
- [4] J. Liu, C.G. Duan, W.G. Yin, W.N. Mei, R.W. Smith, J.R. Hardy, *Phys. Rev. B* **70**, 144106 (2004).
- [5] B. Renner, P. Lunkenheimer, M. Schetter, A. Loidl, A. Reller, S.G. Ebbinghaus, *J. Appl. Phys.* **96**, 4400 (2004).
- [6] D. Szwagierczak, J. Kulawik, *J. Eur. Ceram. Soc.* **28**, 2075 (2008).
- [7] D. Szwagierczak, J. Kulawik, *J. Alloys Comp.* **491**, 465 (2010).

- [8] R. Löhnert, B. Capraro, S. Barth, H. Bartsch, J. Müller, J. Töpfer, *J. Eur. Ceram. Soc.* **35**, 3043 (2015).
- [9] D. Szwagierczak, J. Kulawik, *Acta Phys. Pol. A* **121**, 119 (2012).
- [10] J. Kulawik, D. Szwagierczak, B. Synkiewicz, *Ferroelectrics* **447**, 19 (2013).
- [11] K. Tsuji, W.T. Chen, H. Guo, W.H. Lee, S. Guillemet-Fritsch, C.A. Randall, *J. Appl. Phys.* **121**, 064107 (2017).
- [12] M.A. Rubia, J.J. Reinoso, P. Leret, J.J. Romero, J. Frutos, J.F. Fernández, *J. Eur. Ceram. Soc.* **32**, 71 (2012).
- [13] A.P. Dementjev, O.P. Ivanova, L.A. Vasilyev, A.V. Naumkin, D.M. Nemirovsky, D.Y. Shalaev, *J. Vac. Sci. Technol. A* **12**, 423 (1994).
- [14] R.P. Vasquez, *J. Electron Spectrosc. Relat. Phenom.* **56**, 217 (1991).
- [15] C. Hinnen, C.N. Huong, P. Marcus, *J. Electron Spectrosc. Relat. Phenom.* **73**, 293 (1995).